J Comput Aided Mol Des (2011) 25:555–567
DOI 10.1007/s10822-011-9441-1

Homology modeling, docking and structure-based pharmacophore of inhibitors of DNA methyltransferase

Jakyung Yoo · José L. Medina-Franco

Received: 8 March 2011 / Accepted: 30 May 2011 / Published online: 10 June 2011

Abstract DNA methyltransferase 1 (DNMT1) is an emerging epigenetic target for the treatment of cancer and other diseases. To date, several inhibitors from different structural classes have been published. In this work, we report a comprehensive molecular modeling study of 14 established DNTM1 inhibitors with a herein developed homology model of the catalytic domain of human DNTM1. The geometry of the homology model was in agreement with the proposed mechanism of DNA methylation. Docking results revealed that all inhibitors studied in this work have hydrogen bond interactions with a glutamic acid and arginine residues that play a central role in the mechanism of cytosine DNA methylation. The binding models of compounds such as curcumin and parthenolide suggest that these natural products are covalent blockers of the catalytic site. A pharmacophore model was also developed for all DNMT1 inhibitors considered in this work using the most favorable binding conformations and energetic terms of the docked poses. To the best of our knowledge, this is the first pharmacophore model proposed for compounds with inhibitory activity of DNMT1. The results presented in this work represent a conceptual advance for understanding the protein–ligand interactions and mechanism of action of DNMT1 inhibitors. The insights obtained in this work can be used for the structure-based design and virtual screening for novel inhibitors targeting DNMT1.

Electronic supplementary material The online version of this article (doi:10.1007/s10822-011-9441-1) contains supplementary material, which is available to authorized users.

J. Yoo · J. L. Medina-Franco (✉)
Torrey Pines Institute for Molecular Studies, 11350 SW Village Parkway, Port St. Lucie, FL 34987, USA
e-mail: jmedina@tpims.org

Keywords Cancer · DNMT · Docking · Epigenetics · Homology model · Pharmacophore

Introduction

DNA methylation at the C5-position of cytosine plays important roles for the epigenetic regulation for gene expression and maintenance for genome integrity, such as genomic imprinting and X-chromosome inactivation [1, 2]. Hypermethylation of the promoter CpG islands that lead to transcriptional silencing of tumor suppressor genes is a general feature in all kinds of cancers. Consequently, development of inhibitors of DNA methylation is a new promising strategy for the treatment of cancer, immunodeficiency and brain disorders [2–4].

DNA methylation is catalyzed by DNA methyltransferases (DNMTs). This is a family of enzymes that transfer a methyl group from *S*-adenosyl-L-methionine (AdoMet) to the carbon-5 position of cytosine residues. To date, three types of DNMT have been identified in the human genome, including two de novo methyltransferases (DNMT3A and DNMT3B) and the maintenance methyltransferase (DNMT1), which is the most abundant of the three [5–7]. The protein DNMT3L has high sequence similarity with the DNMT3A enzyme, but it lacks any catalytic activity owing to the absence of conserved catalytic residues. However, DNMT3L is required for the catalytic activity of DNMT3A and 3B [8]. The protein DNMT2 can be found in mammalian cells. Despite the structure of DNMT2 being similar to that of other DNMTs, its role is comparably less understood [9]. It has been reported that DNMT2 does not methylate DNA but instead methylates aspartic acid transfer RNA (tRNAAsp) [10]. More recent experiments suggest that DNMT2 activity is not

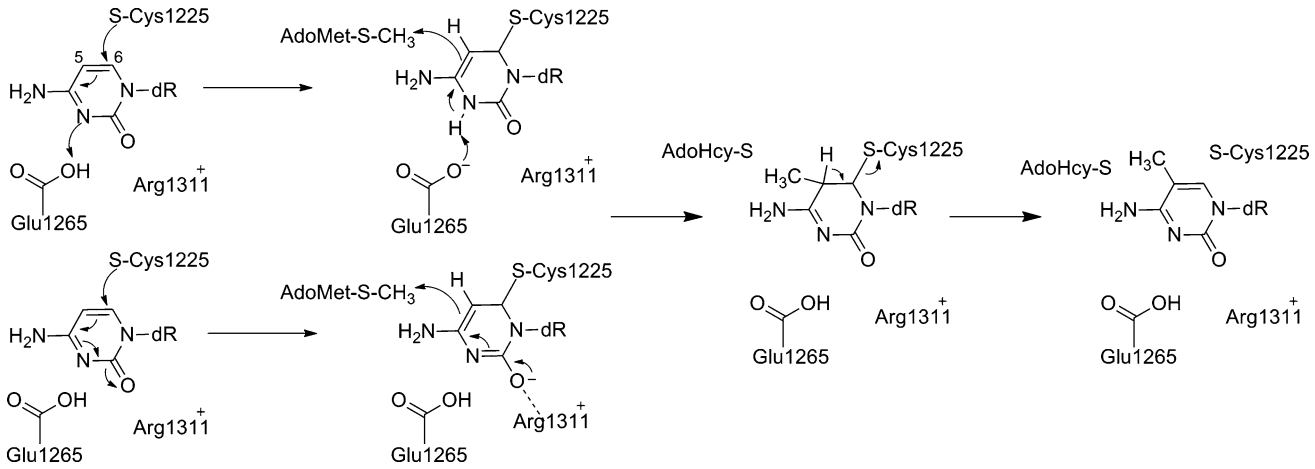

Fig. 1 Mechanism of DNA methylation. Amino acid residue numbers are based on the homology model herein developed. Equivalent residue numbers in the M.HaI crystal structure of residues shown here are Cys81, Glu119, and Arg165

limited to $tRNA^{Asp}$ and that DNMT2 represents a noncanonical enzyme of the DNMT family [9].

Figure 1 shows the proposed mechanism of DNA methylation [11–13]. The DNA cytosine C5 methylation occurs in the catalytic binding site of DNMT1 using AdoMet. The nucleophile attack on the target cytosine C6 by the thiol group of cysteine residue, produces a covalent intermediate between the enzyme and DNA. The activated C5 position of cytosine conducts a nucleophilic attack on the methyl group of the methyl-donating cofactor AdoMet to form the 5-methyl covalent adduct and *S*-adenosyl-L-homocysteine (AdoHcy). The attack on the C6 position is assisted by a transient protonation of the cytosine ring at the endocyclic nitrogen atom N3 which is stabilized by a glutamate residue (Glu1265). The high-energy carbanion may also be stabilized by resonance where an arginine residue (Arg1311) plays an important role in the catalytic mechanism.

To date, several classes of DNMT1 inhibitors have been reported. In this work, DNMT inhibitors are classified into four major groups mainly depending on the associated mechanism of inhibition (Table 1): (1) Nucleoside analogues such as 5-azacytidine [14–18], decitabine [19–23], 5-fluoro-2′-deoxy-cytidine [24, 25], and zebularine [26–30]; (2) non-nucleoside inhibitors and putative covalent blockers. This group includes curcumin [31–33], parthenolide [34–38], and RG108-1 [39], a maleimide analogue of RG108 (vide infra); (3) non-nucleoside and non-covalent blockers such as hydralazine [40–44], procaine [45–47], procainamide [41, 48], (−)-epigallocatechin-3-gallate (EGCG) [49–53], and mahanine [54, 55]; and (4) non-covalent blockers identified from virtual screening such as RG108 [56–58] and NSC14778 [59, 60]. Some of these compounds are drugs approved for other indications such as hydralazine, procaine, and procainamide (vide infra). Curcumin, parthenolide, EGCG, and mahanine are natural products. To date, only 5-azacytidine and decitabine have been developed clinically. These two drugs, after incorporation into DNA, cause covalent trapping and subsequent depletion of DNMT. Aza nucleosides are FDA approved for the treatment of myelodysplastic syndrome, where they demonstrate significant, although usually transient improvement in patient survival and are currently being tested in many solid cancers [16, 61, 62]. Therefore, there is an urgent need to discover and optimize novel DNMT inhibitors. To this end, computational studies are promising to help to elucidate the basic structural requirements of the inhibitors for activity [63]. Indeed, docking models have been proposed for some inhibitors [63]. However, previously reported docking studies were conducted for few ligands using different docking programs, protocols, and different homology models.

The objective of this work was to get insights into the key protein–ligand interactions of DNMT1 inhibitors. To this end, we docked a comprehensive set of DNMT1 inhibitors with a homology model of the catalytic domain of human DNMT1 (hDNMT1). Homology models of hDNMT1 have been useful for the computational study of DNMT1 inhibitors [63]. Here we also propose the first pharmacophore model for DNMT1 inhibitors using a recently developed and validated structure-based approach. The findings of this work will be useful for the virtual screening, structure-based design, and optimization of DNMT1 inhibitors.

Experimental section

Homology model of hDNMT1

The sequence of the human DNMT1 was taken from the UniProt [64] (entry P26358); and the 1133rd to 1601st residues, which correspond to the catalytic domain, were

extracted. The hDNMT1 sequence was aligned based on the sequence of DNA methyltransferases M.HhaI (Protein Data Bank code 6MHT), M.HaeIII (1DCT) and DNMT2 (1G55) and built based on the template 3D structures using Prime (Prime, v2.2, Schrödinger, LLC, New York, NY) [65]. AdoHcy was included in this model, and the DNA double helix was constructed from the structure of M.HhaI. The variable small loops and gaps were filled by knowledge-based homology or ab initio approach of ORCHESTRAR [66], and then the missing long loop was modeled using the Loop Search module implemented in Sybyl 8.0. The loops showing the highest homology and the lowest root mean square deviations were selected. The side chains and hydrogen atoms were added, and the stability of the homology model was validated by checking the geometry using PROCHECK [67]. The homology model coordinates were then energy minimized with Schrödinger Macromodel module (Macromodel, version 9.8, Schrödinger, LLC, New York, NY) using MMFFs force field in a water environment until converging at a termination gradient of 0.05 kJ/mol-Å. The H-bonds were fixed using the SHAKE algorithm during molecular dynamics.

Molecular docking

The starting conformation of ligands was obtained by the Polak-Ribiere Conjugate Gradient (PRCG) energy minimization using the OPLS 2005 force field of 5,000 steps or until the energy difference between subsequent structures was 0.001 kJ/mol-Å [68]. In order to generate the grids for docking, the DNA double helical structure was removed from the homology model of hDNMT1. The target cytidine was used as the reference ligand to generate the grids. The binding site was generated by grids with a default rectangular box centered on the target cytidine. Ligands were docked into the catalytic binding site of hDNMT1 with Glide extra precision (XP) (Glide, version 5.6, Schrödinger, LLC, New York, NY). XP descriptors were generated to obtain atom-level energy terms such as hydrogen bond interaction, electrostatic interaction, hydrophobic enclosure and pi–pi stacking interaction during the docking run. The best docking poses were selected to generate the pharmacophore features.

Structure-based pharmacophore (e-pharmacophore)

The structure-based pharmacophore was generated using the optimized, best scoring pose, and descriptors of the Glide XP score for all 14 inhibitors. To this end, we used the recently developed energy-optimized pharmacophore (e-pharmacophore) approach that is based on mapping of the energetic terms from the Glide XP scoring function onto atom centers [69, 70]. Briefly, the docking models of the inhibitors were refined using Glide XP, the Glide XP scoring terms were computed, and the energies were mapped into atoms. Then, the pharmacophoric sites were automatically generated with Phase (Phase, v3.2, Schrödinger, LLC, New York, NY) using the default set of six chemical features: namely, hydrogen bond acceptor (A), hydrogen bond donor (D), hydrophobic (H), negative ionizable (N), positive ionizable (P), and aromatic ring (R) site. The Glide XP energies from the atoms that comprise each pharmacophoric site were summed. The pharmacophoric sites were then ranked based on the summed energies, and the most favorable sites were selected for the pharmacophore hypothesis. Further details of the e-pharmacophore method are published elsewhere [69, 70]. In other words, each pharmacophore feature was assigned with an energetic value that was the sum of the Glide XP contributions of the atoms comprising the site. The sites were quantified and ranked on the basis of these energetic terms [69, 70]. These features were used to develop a common pharmacophore model that was evaluated on its ability to reproduce known inhibitors using Phase. The distance matching tolerance was set to 2.0 Å. To account for protein flexibility and lessen the effects of minor steric clashes, excluded volumes spheres were created for all receptor atoms within 5 Å around each ligand. Each sphere has a radius corresponding to 50% of the van der Waals radius of the receptor atom. Receptor atoms less than 1.5 Å from the ligand were ignored. The combination of best-scoring features that matched a minimum of two sites in each known inhibitor were chosen and regenerated [69, 70].

Results and discussion

Homology model of the catalytic domain of hDNMT1

The homology model of the catalytic binding site of hDNMT1 herein developed was consistent with the mechanism of DNA methylation (Fig. 2a). The target cytidine (adopted from the HhaI-DNA structure) is located between the nucleophile Cys1225 and sulfur atom of AdoHcy (Fig. 2b). The distance of cytosine C6 to the sulfur atom of Cys1225 is 3.3 Å. The cytosine C5 atom is 3.0 Å away from the sulfur atom of AdoHcy. In addition, the N3 protonated form of cytosine can make hydrogen bonds with Glu1265, Arg1311, and Pro1223. This is in full agreement with the proposed catalytic mechanism of DNA methylation (Fig. 1). The α-phosphate backbone of deoxycytidine makes a hydrogen bond network with Arg1311, Ser1229, and Gly1230. In addition, the 3′-OH of the sugar moiety forms hydrogen bonds with Arg1461 and Gln1396. The geometry of the catalytic site suggests that the homology

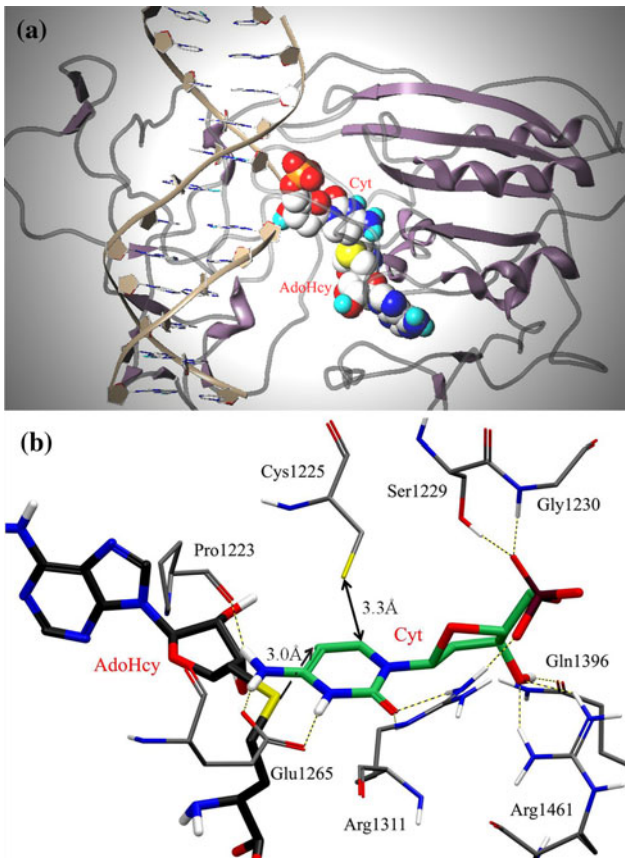

Fig. 2 **a** Homology model of hDNMT1-AdoHcy-DNA. Cytidine and AdoHcy are shown as space-filling (CPK) models; hDNMT1 is shown as ribbons. **b** Binding mode of N3 protonated deoxycytidine (carbon atoms in *green*) in the catalytic domain of hDNMT1 (carbon atoms in *gray*). AdoHcy (carbon atoms in *black*) is shown for reference. See the online version of the manuscript for colors

model of hDNMT1 is reliable to *explore* the binding mode of hDNMT1 inhibitors.

Molecular docking

Fourteen established known hDNMT1 inhibitors (Table 1) were docked into the optimized catalytic binding site of the homology model. The docking models of the DNMT1 inhibitors are discussed in four major sections following the classification presented in Table 1. It is worth pointing out that there are no reports of the enzymatic inhibitory activity of the 14 inhibitors tested under the same assay conditions. Therefore, a direct correlation between docking scores (Table S1 in the Supplementary data) and enzymatic activity is not representative.

Nucleoside analogues

Figure 3 shows the docked poses of selected nucleoside inhibitors e.g., cytosine analogues, 5-azacytidine, and zebularine. The binding mode of 5-azacytidine closely matches with the target cytidine (Fig. 3a). Similar binding poses were obtained for zebularine, decitabine, and 5-fluoro-2′-deoxycytidine (Fig. S1 in the Supplementary data). This is consistent with their high structural similarity. According to these binding models, the α-phosphate and ribose groups make a hydrogen bond network with Arg1311, Arg1461, Gln1396, Ser1229, and Gly1230. Most of the nucleoside inhibitors make key interactions with the side chains of Glu1265 and Arg1311. Although zebularine does not have an amino group at the C4 position and, consequently, does not form hydrogen bonds with Glu1265 and Pro1223, the covalent bond distance between Cys1225 and C6 is sufficient to start the catalytic mechanism (Fig. 3b). In addition, the N3 of zebularine and $O^{\varepsilon 1}$ of Glu1265 are within hydrogen bonding distance for N3 protonation (Fig. 3b). These observations are in agreement with the X-ray structure for zebularine in the catalytic site of bacterial methyltransferase (M.HhaI) [71].

Non-nucleoside and putative covalent blockers

Curcumin has several pharmacological properties including antitumor, anti-inflammatory, anti-angiogenic, antioxidant, and wound healing [72]. Based on docking studies with Autodock using a homology model of hDNMT1, Liu et al. recently suggested that curcumin covalently blocks the thiolate of catalytic cysteine of DNMT1 [33]. This observation is largely in part because of the α,β-unsaturated carbonyl group of curcumin. In this work, we further examined the binding mode of curcumin with Glide using the herein developed homology model of the catalytic domain of hDNMT1. Figure 4a shows the binding mode of curcumin. According to this model, one of the 4-hydroxy-3-methoxyphenyl groups occupies a similar binding position as the base ring of 5-azacytidine and forms hydrogen bonds with Glu1265 and Arg1311. Moreover, the diketone groups of curcumin make hydrogen bonds with the side chains of Gln1226 and Lys1462. In this binding position, the α,β-unsaturated carbonyl is 2.8 and 3.3 Å away from the sulfur atom of catalytic Cys1225. The other 4-hydroxy-3-methoxyphenyl group of curcumin forms a hydrogen bond with the side chain of His1458 and the carbonyl backbone of Leu1454. This result supports the hypothesis that curcumin has the potential to inhibit the DNMT1 catalytic function through covalently blocking the catalytic thiolate of Cys1225. Furthermore, this result is in good agreement with the docking studies reported previously by Liu et al. [33] despite the fact that we used a different homology model and docking protocol.

The sesquiterpene lactone parthenolide is found in the anti-inflammatory medicinal herb feverfew. Parthenolide has reported inhibitory activity of the nuclear transcription

Table 1 Inhibitors of DNA methylation considered in this study

Compound	Structure	Target(s)	Testing Stage	References
Nucleoside analogues				
5-Azacytidine	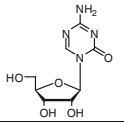	DNMT1, other enzymes	Approved by FDA in 2004; Pharmion Corp.	[14-18]
Decitabine	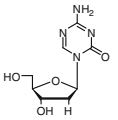	DNMTs	Approved by FDA in 2006; MGI Pharma	[19-23]
Zebularine	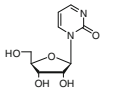	DNMT1, other enzymes	Preclinical	[26-30]
5-Fluoro-2′-deoxycytidine	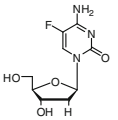	DNMTs	Phase I	[24,25]
Non-nucleoside and putative covalent blockers				
Curcumin	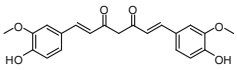	DNMT1, other enzymes	Phase I: Breast cancer Phase II: Pancreatic cancer	[31-33]
Parthenolide	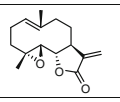	DNMT1, other enzymes	Phase I: anti-tumor anti-angiogenic Preclinical: Anti-inflammatory	[34-38]
RG108-1	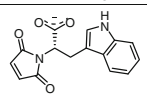	hDNMT1	*In vitro*	[39]
Non-covalent blockers				
Hydralazine	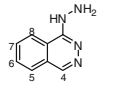	DNMTs	Phase II: Breast cancer Phase III: Cervical and ovarian cancer	[40-44]
Procaine	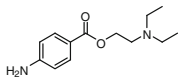	DNMTs / CpG-rich sequences	Phase II	[45-47]
Procainamide	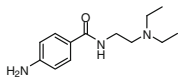	DNMTs / CpG-rich sequences	Preclinical	[41,48]
EGCG	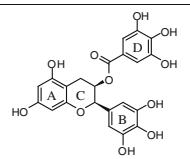	DNMT1, other enzymes	Phase I	[49-53]
Mahanine	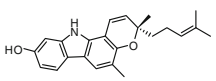	DNMTs	*In vitro:* Human prostate cancer cells	[54,55]
Non-covalent blockers identified from virtual screening				
RG108	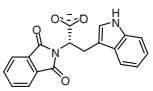	DNMTs	Preclinical	[56-58]
NSC14778	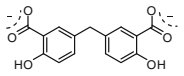	DNMT1, other enzymes	*In vitro*: Human and dengue virus methyltransferase	[59,60]

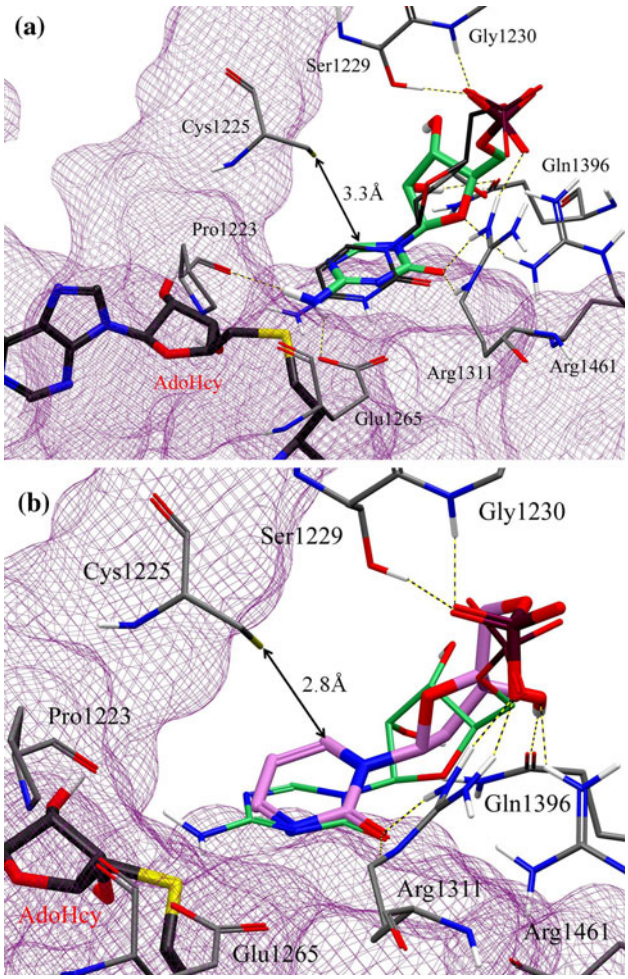

Fig. 3 Comparison of binding modes of nucleoside inhibitors, **a** 5-azacytidine (carbon atoms in *green*) with deoxycytidine (carbon atoms in *dark gray*) and **b** zebularine (carbon atoms in *pink*). See the online version of the manuscript for colors

factor (NF-κB) through covalent blocking the thiol group of cysteine in the active site of NF-κB [34–36]. This natural product also has been identified as an effective hypomethylating agent. Previous docking studies with DNMT1 suggested that parthenolide covalently blocks the DNMT1 active site [38]. To further support this hypothesis, we docked this compound using our homology model. Figure 4b shows the optimized binding pose of parthenolide using Glide XP. In this binding model, the methylene atom of parthenolide is 2.9 Å away from the sulfur atom of the catalytic Cys1225. This is in agreement with the putative formation of a covalent adduct between DNMT and parthenolide. Indeed, the methylene atom of parthenolide overlaps with the C6 atom of the base ring of 5-azacytidine. This natural product also forms hydrogen bonds with three arginine residues namely Arg1311, Arg1309, and Arg1461.

RG108-1 (Table 1) is a maleimide analogue of RG108 (vide infra). Suzuki et al. [39] previously docked RG108-1

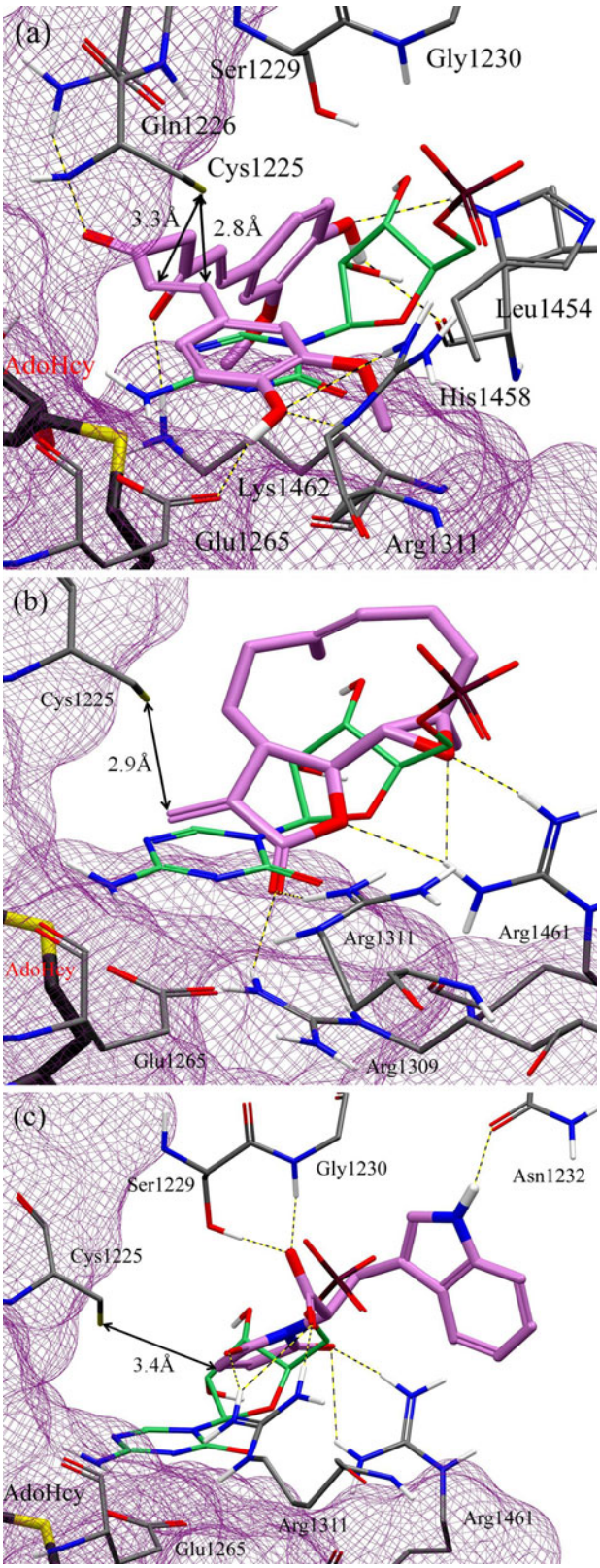

Fig. 4 Comparison of the binding modes of putative covalent blockers (carbon atoms in *pink*), **a** curcumin, **b** parthenolide, and **c** RG108-1 with 5-azacytidine (carbon atoms in *green*). See the online version of the manuscript for colors

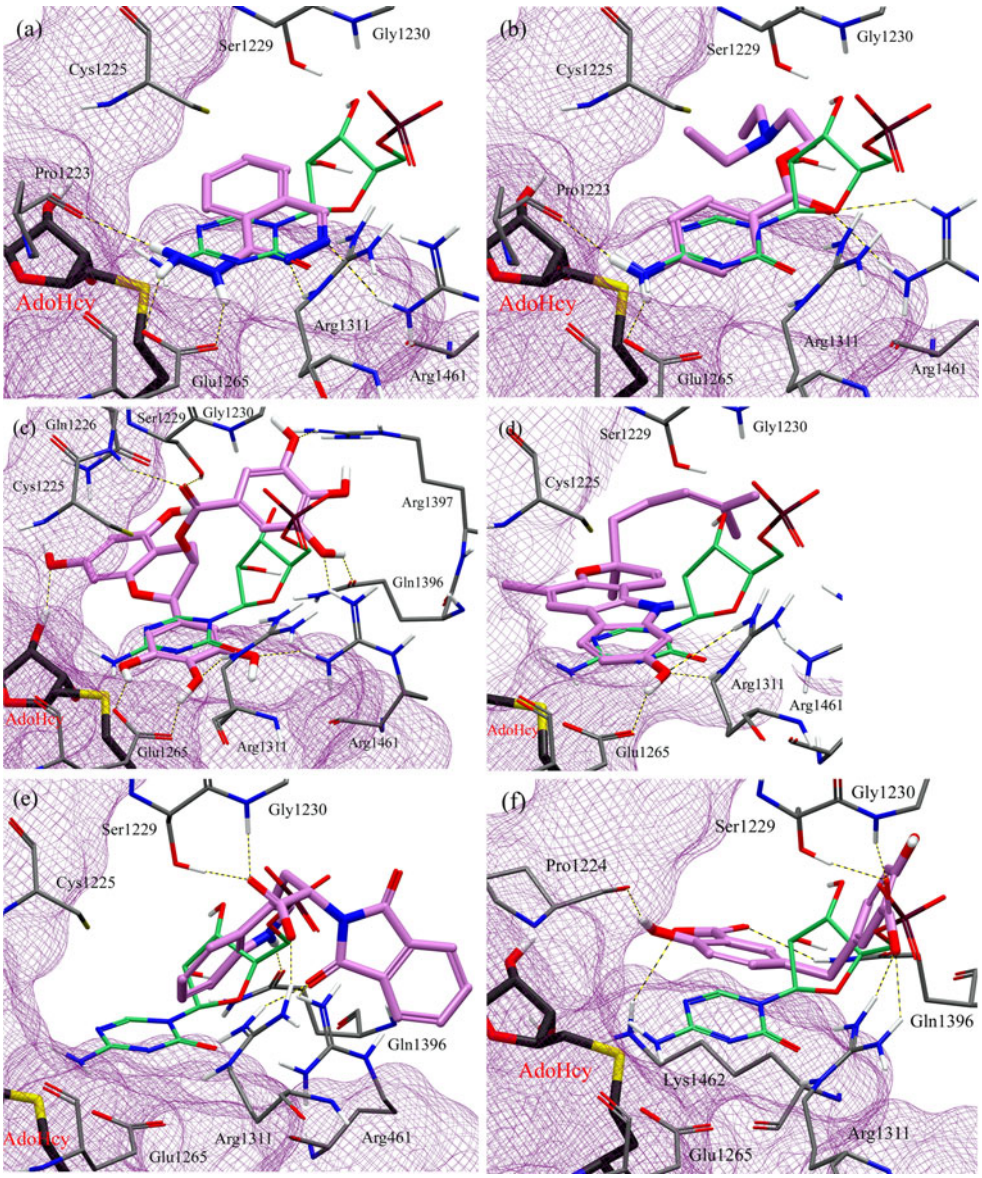

Fig. 5 Comparison of the binding modes of non-covalent blockers (carbon atoms in *pink*) with 5-azacytidine (carbon atoms in *green*). Drugs used in other indications: **a** hydralazine and **b** procaine; Natural products: **c** EGCG and **d** mahanine; Virtual screening hits: **e** RG108 and **f** NSC14778. See the online version of the manuscript for colors

with an X-ray structure of bacterial M.HhaI concluding that this maleimide derivative may act as a covalent blocker. Herein, we further tested this hypothesis but using a model of the human DNMT1. Figure 4c shows a comparison of the binding model of RG108-1 with 5-azacytidine that is displayed as a reference. The carboxylate anion of RG108-1 overlaps with the phosphate anion of 5-azacytidine and has the same interaction with Arg1311, Ser1229, and Gly1230. Interestingly, the maleimide moiety of RG108-1 interacts with Arg1311 and Arg1461 and lies across the sugar ring of 5-azacytidine, where the conjugate addition of a thiol to the maleimide can occur. The indole ring of RG108-1 forms a hydrogen bond with Asn1232. These results further supports the previous hypothesis that RG108-1 is a covalent blocker of hDNMT1.

Non-covalent blockers

Hydralazine is an antihypertensive drug. Using a drug repurposing strategy [73], clinical trials have demonstrated the antitumor effect of the combination of hydralazine with valporic acid (a histone deacetylase inhibitor) [74]. Figure 5a shows the comparison of the binding modes of hydralazine with 5-azacytidine. The amino group of hydralazine matched well with the amino group of 5-azacytidine, and it is capable of forming a hydrogen bond with Glu1265 and Pro1223. The nitrogen of the phthalazine ring overlapped with the carbonyl oxygen of 5-azacytidine and formed hydrogen bonds with Arg1311 and Arg1461. This result also suggests that hydralazine can be substituted at the C4 position (Table 1) to yield analogues with enhanced

affinity with the enzyme. Similar conclusions were obtained using a different homology model and docking program [44].

Procaine and procainamide are approved drugs as local anesthetic and for the treatment of cardiac arrhythmias [17, 48], respectively. Figure 5b shows the binding mode of procaine. The binding mode of procainamide was the same (Fig. S1 in the Supplementary data). The amino group of procaine overlapped with that of 5-azacytidine and made a hydrogen bond with Glu1265 and Pro1223. Moreover, the carbonyl oxygen of these two ligands was close to the binding position of oxygen of the ribose ring of 5-azacytidine making a similar hydrogen bond with Arg1461.

Figure 5c shows the binding mode of EGCG, the main polyphenolic component of green tea. According to this binding model, the B ring of EGCG (Table 1) was oriented at the same position as the base ring of 5-azacytidine forming hydrogen bonds with Glu1265 and Arg1311, residues relevant in the mechanism of methylation. Arg1461 stabilize the B and D ring through hydrogen bonds with the hydroxy atoms of the two rings. The D ring makes interactions with Gln1396 and Arg1397. The ketone group of EGCG forms hydrogen bonds with the backbone of Gln1226 and the hydroxy group of the side chain of Ser1229. Interestingly, the hydroxy group of the A ring forms a hydrogen bond with the 2′-OH of the sugar ring of AdoHcy. These findings suggest that EGCG inhibits DNMT1 by blocking the catalytic active site. The overall binding conformation of EGCG is slightly different from the previously reported binding mode using a different homology model and docking method [49, 75]. However, the published models also predict the formation of hydrogen bonds with Ser1229, Glu1265, and Arg1309.

The antiproliferative effect of mahanine, a naturally occurring carbazole alkaloid, has been associated with the inhibition of DNMT activity [54]. The docking study of mahanine in the active site of DNMT is not published. Figure 5d shows the binding mode of mahanine within the catalytic site of hDNMT1. The binding model is characterized by the formation of hydrogen bonds with key amino acid residues, Glu1265 and Arg1311.

RG108 is a novel DNMT inhibitor that was discovered by docking-based virtual screening of the National Cancer Institute (NCI) database using a homology model of hDNMT [58]. RG108 was reported to induce the re-expression of different hypermethylation silenced genes, such as p16 and the putative tumor suppressor genes SRFP1 and TIMP-3, in colon cancer cells [56]. Figure 5e shows the binding model of RG108 obtained with our homology model. 5-Azacytidine is displayed for reference. The carbonyl atom of the phthalimide ring of RG108 forms hydrogen bonds with Arg1311 and Arg1461. The NH of the indole ring interacts with Gln1396 in a similar manner as the 2′-OH of the sugar moiety of 5-azacytidine. In addition, the carboxylate anion of RG108 roughly overlaps with the phosphate anion of 5-azacytidine having a similar hydrogen bond pattern with Arg1311, Ser1229, and Gly1230. The binding mode of RG108 proposed with our homology model is similar to the binding mode previously reported with a different homology model [58]. A comparison with the binding mode of RG108 and RG108-1 is shown in the Supplementary data (Fig. S2). The carboxylate anions of both compounds overlap. The phthalimide group of RG108 is positioned in the same binding site as the indole ring of RG108-1.

NSC14778 was identified as a novel inhibitor of DNMT1 also by virtual screening of the NCI database [59]. Figure 5f shows the optimized docked model of NSC14778 in the active site. 5-Azacytidine is shown as reference. One of the carboxylate groups makes a hydrogen bond network with the side chains of Arg1311, Ser1229, and Gly1230. This group mimics the interaction of the phosphate of 5-azacytidine. The second hydroxybenzoic acid moiety has contacts with Lys1462, Pro1224, and Gln1396. These observations suggest that NSC14778 might block the active site of DNMT1 non-covalently.

Despite the fact the inhibitors studied in this work involve a range of different scaffolds and alternative binding modes could be possible, the binding models of the 14 hDNMT1 inhibitors showed common hydrogen bond interactions with Arg1311 or Glu1265. These two residues are key amino acids in the mechanism of cytosine DNA methylation (Fig. 1). In addition, several inhibitors also form hydrogen bonds with at least one of the following residues Arg1461, Ser1229 or Gly1230. These results *suggest* that interactions with these residues are pharmacophoric. The specific effects of the inhibitors on the side-chain rearrangements and conformation of the catalytic site of hDNMT1 remain to be determined in a comprehensive manner, for example, using molecular dynamics.

Structure-based pharmacophore hypothesis

As noted above, a number of inhibitors investigated in this work can be classified into different structural classes e.g., nucleosides and non-nucleosides. It would be interesting to explore specific pharmacophoric models for each class of inhibitor depending on the proposed mechanism of action (Table 1). Since all the 14 inhibitors showed common interactions in the docking models with hDNMT1, in this work we decided to develop a pharmacophoric model for all inhibitors that further characterizes the major interactions involved in the ligand–protein recognition process. To develop a pharmacophore hypothesis of the 14 DNMT1 inhibitors, we employed the e-pharmacophore method recently developed and summarized in the "Experimental

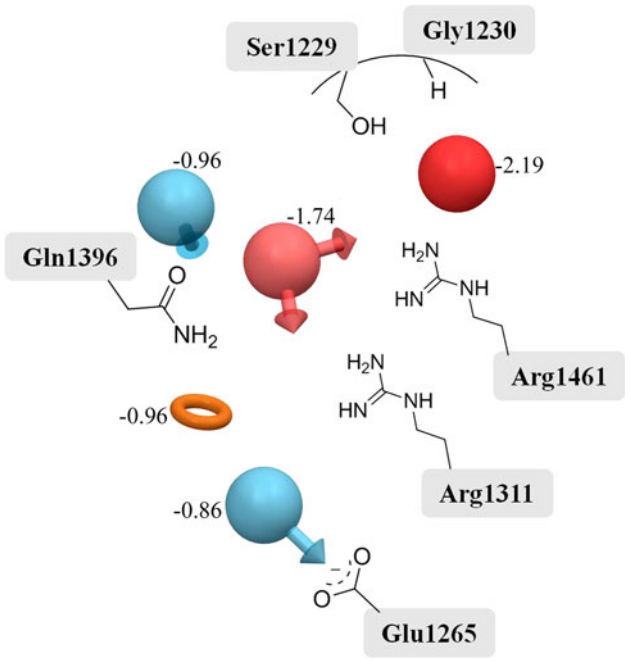

Fig. 6 Structure-based pharmacophore model for DNMT inhibitors. *Red sphere* negative ionizable, *pink sphere* hydrogen bond acceptor, *blue sphere* hydrogen bond donors, and *orange ring* aromatic ring. Selected amino acid residues in the catalytic site are schematically depicted for reference. See the online version of the manuscript for colors

section". This method has the advantage of combining pharmacophore perception with protein–ligand energetic terms, computed with docking, to rank the importance of the pharmacophore features [69, 70]. The best scoring poses and energetic information of the 14 known inhibitors were taken from the docking studies described above. Figure 6 shows the five-feature pharmacophore model for the 14 DNMT1 inhibitors. The energetic value assigned to each pharmacophoric feature is displayed in the figure. The energetic value is equal to the sum of the Glide XP contributions of the atoms comprising the site [70]. Nearby amino acids are schematically depicted for reference. The best-scoring feature is a negative charge which is close to the side chains of Ser1229, Gly1230, and Arg1311. The second most favorable feature is an acceptor site that is in close proximity with the side chains of Arg1311 and Arg1461. The third ranked features are an aromatic ring that stabilizes the binding conformation of ligands between AdoHcy and Cys1225, and a donor site that is close to the side chain of Gln1396. The fifth-ranked feature is a donor site that is nearby the side chain of Glu1265, which is a residue implicated in the methylation mechanism (Fig. 1). The pharmacophore model captures the most important interactions of the 14 DNMT inhibitors. To note, glutamic acid and arginine residues are highly conserved residues in catalytic domains of investigated DNMTs [76]. Figure 7 shows the alignment of representative inhibitors to the pharmacophore hypothesis. Most of the inhibitors matched several pharmacophore features considering a distance tolerance of 2 Å as detailed in the next paragraphs.

The nucleoside analogues, 5-azacytidine, decitabine, and 5-fluoro-2′-deoxycytidine matched with all five pharmacophore features. In comparison, zebularine matches four. This is because zebularine does not have the amine group on the base ring and does not satisfy the hydrogen bonding donor feature associated with the interaction with Glu1265. However, the donor feature can match the N3 protonated form of zebularine (Fig. 7).

Curcumin, procaine, procainamide, and hydralazine matched with the aromatic ring, donor, and acceptor features. Despite the fact hydralazine is a very small structure, the amine atoms of this molecule match with acceptor and donor features that are close to Glu1265 and Arg1311. The B ring of EGCG satisfied both the aromatic ring and the donor nearby Glu1265. The hydroxy group of the D ring matched with the donor close to Gln1396, and the acceptor. The carboxylate anions of RG108, RG108-1, and NSC14778 matched with the negative feature. The maleimide of RG108-1 satisfied the acceptor, while the indole ring matched with the donor that is close to Gln1396 (Fig. 7).

Although NSC14778 matched with only one pharmacophoric feature, its carboxylate group matched with the best-scored feature, i.e., the negative charge. This model suggests that introduction of a substituent that could match the donor feature associated with the interaction of Glu1265 and acceptor feature may enhance the affinity of NSC14778 with the enzyme. Parthenolide also matched with only one feature, namely, the acceptor site associated with the interaction with Arg1311 and Arg1461. Interestingly, it is possible that the enol form of parthenolide interacts with Glu1265 when the keto-enol tautomerism on the γ-methylene lactone ring occurs through covalent linking with catalytic Cys1225.

These results suggest that the structure-based pharmacophore in Fig. 6 has good agreement with docking studies and represents a key step towards the understanding of the protein–ligand interactions of DNMT1 inhibitors, which is the main goal of this work (vide supra). It remains to evaluate the performance of the pharmacophore model in prospective virtual screening. In such studies, virtual screened molecules could be required to match at least three or four e-pharmacophoric sites [70]. These studies are ongoing in our group and will be reported in due course.

Conclusion

In the present study, we explored the binding mode of 14 DNMT1 inhibitors with a herein developed homology

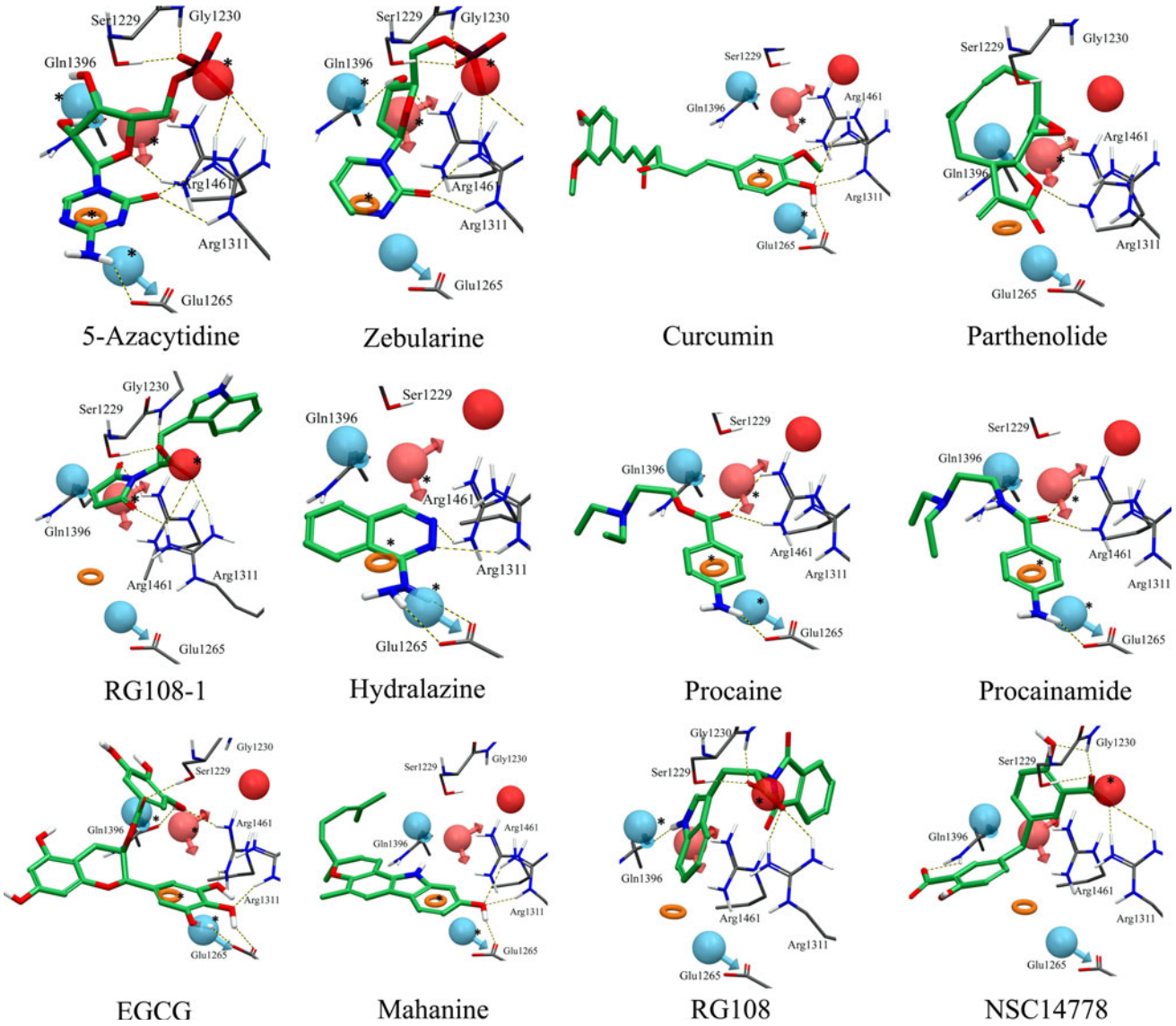

Fig. 7 Comparison between the binding mode and pharmacophore hypothesis for representative DNMT inhibitors. *Red sphere* negative ionizable, *pink sphere* hydrogen bond acceptor, *blue sphere* hydrogen bond donors, and *orange ring* aromatic ring. The *asterisk* denotes the matching site with the inhibitors. Selected amino acid residues in the catalytic site are shown for reference. See the online version of the manuscript for colors

model of the catalytic domain of hDNMT1. To the best of our knowledge, this is the first study that compares the binding mode of all the inhibitors using the same molecular modeling protocol. The geometry of the homology model was in agreement with the proposed mechanism of DNA methylation. The catalytic site of the homology model includes the residues Cys1225, Glu1265, and Arg1311. Despite the fact that the inhibitors studied in this work have different structural scaffolds, all compounds have common interactions with key amino acid residues such as Glu1265, Arg1311, Arg1461, Ser1229, and Gly1230. The nucleoside analogues, such as 5-azacytidine, decitabine, 5-fluoro-2′-deoxycytidine, and zebularine, have several interactions with more than five amino acid residues and showed a similar binding position as the modeled cytidine. These results further supported the use of the homology model to explore the binding modes of other inhibitors. Docking results also supported the hypothesis that curcumin, parthenolide, and a maleimide analogue of RG108 are covalent blockers of the catalytic cysteine. The optimized binding modes of the inhibitors were used to construct a structure-based pharmacophore model with five distinct features: namely, one negative charge, one hydrogen bond acceptor, one aromatic ring, and two hydrogen bond donors. The pharmacophore model is in agreement with the binding profile of the inhibitors obtained in docking. Taken

together, the results of this study shed light into the key protein–ligand interactions of the DNMT1 inhibitors. A major perspective of this work is to apply the insights from the docking and pharmacophore model obtained in this work for the virtual screening and structure-based optimization of novel DNMT inhibitors.

Acknowledgments Authors thank Dr. Fabian López-Vallejo and Dr. Thomas Caulfield for helpful discussions. We also thank Karen Gottwald for proofreading the manuscript. This work was supported by the Menopause & Women's Health Research Center and the State of Florida, Executive Office of the Governor's Office of Tourism, Trade, and Economic Development.

References

1. Jones PA, Baylin SB (2002) The fundamental role of epigenetic events in cancer. Nat Rev Genet 3:415–428
2. Robertson KD (2005) DNA methylation and human disease. Nat Rev Genet 6:597–610
3. Miller CA, Gavin CF, White JA, Parrish RR, Honasoge A, Yancey CR, Rivera IM, Rubio MD, Rumbaugh G, Sweatt JD (2010) Cortical DNA methylation maintains remote memory. Nat Neurosci 13:664–666
4. Zawia NH, Lahiri DK, Cardozo-Pelaez F (2009) Epigenetics, oxidative stress, and Alzheimer disease. Free Radical Biol Med 46:1241–1249
5. Bestor T, Laudano A, Mattaliano R, Ingram V (1988) Cloning and sequencing of a cDNA encoding DNA methyltransferase of mouse cells: the carboxyl-terminal domain of the mammalian enzymes is related to bacterial restriction methyltransferases. J Mol Biol 203:971–983
6. Okano M, Xie S, Li E (1998) Cloning and characterization of a family of novel mammalian DNA (cytosine-5) methyltransferases. Nat Genet 19:219–220
7. Bacolla A, Pradhan S, Roberts RJ, Wells RD (1999) Recombinant human DNA (cytosine-5) methyltransferase. II. Steady-state kinetics reveal allosteric activation by methylated DNA. J Biol Chem 274:33011–33019
8. Cheng X, Blumenthal RM (2008) Mammalian DNA methyltransferases: a structural perspective. Structure 16:341–350
9. Schaefer M, Lyko F (2009) Solving the Dnmt2 enigma. Chromosoma 119:35–40
10. Goll MG, Kirpekar F, Maggert KA, Yoder JA, Hsieh CL, Zhang X, Golic KG, Jacobsen SE, Bestor TH (2006) Methylation of $tRNA^{Asp}$ by the DNA methyltransferase homolog Dnmt2. Science 311:395–398
11. Kumar S, Horton JR, Jones GD, Walker RT, Roberts RJ, Cheng X (1997) DNA containing 4′-thio-2′-deoxycytidine inhibits methylation by HhaI methyltransferase. Nucleic Acids Res 25:2773–2783
12. Jurkowski TP, Meusburger M, Phalke S, Helm M, Nellen W, Reuter G, Jeltsch A (2008) Human DNMT2 methylates $tRNA^{Asp}$ molecules using a DNA methyltransferase-like catalytic mechanism. RNA 14:1663–1670
13. Hermann A, Gowher H, Jeltsch A (2004) Biochemistry and biology of mammalian DNA methyltransferases. Cell Mol Life Sci 61:2571–2587
14. Sorm F, Píškala A, Cihák A, Veselý J (1964) 5-Azacytidine, a new, highly effective cancerostatic. Experientia 20:202–203
15. Jones PA, Taylor SM (1980) Cellular differentiation, cytidine analogs and DNA methylation. Cell 20:85–93
16. Kaminskas E, Farrell AT, Wang YC, Sridhara R, Pazdur R (2005) FDA drug approval summary: azacitidine (5-azacytidine, vidaza™) for injectable suspension. Oncologist 10:176–182
17. Yu N, Wang M (2008) Anticancer drug discovery targeting DNA hypermethylation. Curr Med Chem 15:1350–1375
18. Amatori S, Bagaloni I, Donati B, Fanelli M (2010) DNA demethylating antineoplastic strategies: a comparative point of view. Genes Cancer 1:197–209
19. Dacogen (2006) Decitabine: FDA approves new treatment for myelodysplastic syndromes (MDS). http://www.fda.gov/bbs/topics/NEWS/2006/NEW01366.html. Accessed 10 May 2011
20. Kantarjian H, Issa JP, Rosenfeld CS, Bennett JM, Albitar M, DiPersio J, Klimek V, Slack J, de Castro C, Ravandi F, Helmer R III, Shen L, Nimer SD, Leavitt R, Raza A, Saba H (2006) Decitabine improves patient outcomes in myelodysplastic syndromes. Cancer 106:1794–1803
21. Palii SS, Van Emburgh BO, Sankpal UT, Brown KD, Robertson KD (2007) DNA methylation inhibitor 5-aza-2′-deoxycytidine induces reversible genome-wide DNA damage that is distinctly influenced by DNA Methyltransferases 1 and 3B. Mol Cell Biol 28:752–771
22. Ferguson AT, Vertino PM, Spitzner JR, Baylin SB, Muller MT, Davidson NE (1997) Role of estrogen receptor gene demethylation and DNA methyltransferase DNA adduct formation in 5-aza-2′-deoxycytidine-induce cytotoxicity in human breast cancer cells. J Biol Chem 272:32260–32266
23. Appleton K, Mackay HJ, Judson I, Plumb JA, McCormick C, Strathdee G, Lee C, Barrett S, Reade S, Jadayel D, Tang A, Bellenger K, Mackay L, Setanoians A, Schätzlein A, Twelves C, Kaye SB, Brown R (2007) Phase I and pharmacodynamic trial of the DNA methyltransferase inhibitor decitabine and carboplatin in solid tumors. J Clin Oncol 25:4603–4609
24. Beumer JH, Parise RA, Newman EM, Doroshow JH, Synold TW, Lenz HJ, Egorin MJ (2008) Concentrations of the DNA methyltransferase inhibitor 5-fluoro-2′-deoxycytidine (FdCyd) and its cytotoxic metabolites in plasma of patients treated with FdCyd and tetrahydrouridine (THU). Cancer Chemother Pharmacol 62:363–368
25. Beumer JH, Eiseman JL, Parise RA, Joseph E, Holleran JL, Covey JM, Egorin MJ (2006) Pharmacokinetics, metabolism, and oral bioavailability of the DNA methyltransferase inhibitor 5-fluoro-2′-deoxycytidine in mice. Clin Cancer Res 12:7483–7491
26. Ben-Kasus T, Ben-Zvi Z, Marquez V, Kelley J, Agbaria R (2005) Metabolic activation of zebularine, a novel DNA methylation inhibitor, in human bladder carcinoma cells. Biochem Pharmacol 70:121–133
27. Bradbury J (2004) Zebularine: a candidate for epigenetic cancer therapy. Drug Discovery Today 9:906–907
28. Cheng JC, Yoo CB, Weisenberger DJ, Chuang J, Wozniak C, Liang G, Marquez VE, Greer S, Orntoft TF, Thykjaer T, Jones PA (2004) Preferential response of cancer cells to zebularine. Cancer Cell 6:151–158
29. Holleran JL, Parise RA, Joseph E, Eiseman JL, Covey JM, Glaze ER, Lyubimov AV, Chen YF, D'Argenio DZ, Egorin MJ (2005) Plasma pharmacokinetics, oral bioavailability, and interspecies scaling of the DNA methyltransferase inhibitor, zebularine. Clin Cancer Res 11:3862–3868
30. Scott SA, Lakshimikuttysamma A, Sheridan DP, Sanche SE, Geyer CR, DeCoteau JF (2007) Zebularine inhibits human acute myeloid leukemia cell growth in vitro in association with p15INK4B demethylation and reexpression. Exp Hematol 35:263–273
31. Bayet-Robert M, Kwiatkowski F, Leheurteur M, Gachon F, Planchat E, Abrial C, Mouret-Reynier MA, Durando X, Barthomeuf C, Chollet P (2010) Phase I dose escalation trial of

docetaxel plus curcumin in patients with advanced and metastatic breast cancer. Cancer Biol Ther 9:8–14
32. Dhillon N, Aggarwal BB, Newman RA, Wolff RA, Kunnumakkara AB, Abbruzzese JL, Ng CS, Badmaev V, Kurzrock R (2008) Phase II trial of curcumin in patients with advanced pancreatic cancer. Clin Cancer Res 14:4491–4499
33. Liu Z, Xie Z, Jones W, Pavlovicz R, Liu S, Yu J, Li P, Lin J, Fuchs J, Marcucci G (2009) Curcumin is a potent DNA hypomethylation agent. Bioorg Med Chem Lett 19:706–709
34. Garciapineres A, Lindenmeyer M, Merfort I (2004) Role of cysteine residues of p65/NF-κB on the inhibition by the sesquiterpene lactone parthenolide and N-ethyl maleimide, and on its transactivating potential. Life Sci 75:841–856
35. Kwok B, Koh B, Ndubuisi M, Elofsson M, Crews C (2001) The anti-inflammatory natural product parthenolide from the medicinal herb Feverfew directly binds to and inhibits IκB kinase. Chem Biol 8:759–766
36. Steele AJ, Jones DT, Ganeshaguru K, Duke VM, Yogashangary BC, North JM, Lowdell MW, Kottaridis PD, Mehta AB, Prentice AG, Hoffbrand AV, Wickremasinghe RG (2006) The sesquiterpene lactone parthenolide induces selective apoptosis of B-chronic lymphocytic leukemia cells in vitro. Leukemia 20: 1073–1079
37. Curry EA III, Murry DJ, Yoder C, Fife K, Armstrong V, Nakshatri H, O'Connell M, Sweeney CJ (2004) Phase I dose escalation trial of feverfew with standardized doses of parthenolide in patients with cancer. Invest New Drugs 22:299–305
38. Liu Z, Liu S, Xie Z, Pavlovicz RE, Wu J, Chen P, Aimiuwu J, Pang J, Bhasin D, Neviani P, Fuchs JR, Plass C, Li PK, Li C, Huang TH, Wu LC, Rush L, Wang H, Perrotti D, Marcucci G, Chan KK (2009) Modulation of DNA methylation by a sesquiterpene lactone parthenolide. J Pharmacol Exp Ther 329:505–514
39. Suzuki T, Tanaka R, Hamada S, Nakagawa H, Miyata N (2010) Design, synthesis, inhibitory activity, and binding mode study of novel DNA methyltransferase 1 inhibitors. Bioorg Med Chem Lett 20:1124–1127
40. Daiber A, Oelze M, Coldewey M, Kaiser K, Huth C, Schildknecht S, Bachschmid M, Nazirisadeh Y, Ullrich V, Mülsch A, Münzel T, Tsilimingas N (2005) Hydralazine is a powerful inhibitor of peroxynitrite formation as a possible explanation for its beneficial effects on prognosis in patients with congestive heart failure. Biochem Biophys Res Commun 338:1865–1874
41. Segura-Pacheco B, Trejo-Becerril C, Perez-Cardenas E, Taja-Chayeb L, Mariscal I, Chavez A, Acuña C, Salazar AM, Lizano M, Dueñas-Gonzalez A (2003) Reactivation of tumor suppressor genes by the cardiovascular drugs hydralazine and procainamide and their potential use in cancer therapy. Clin Cancer Res 9:1596–1603
42. Zambrano P, Segura-Pacheco B, Perez-Cardenas E, Cetina L, Revilla-Vazquez A, Taja-Chayeb L, Chavez-Blanco A, Angeles E, Cabrera G, Sandoval K, Trejo-Becerril C, Chanona-Vilchis J, Duenas-González A (2005) A phase I study of hydralazine to demethylate and reactivate the expression of tumor suppressor genes. BMC Cancer 5:44
43. Candelaria M, Gallardo-Rincón D, Arce C, Cetina L, Aguilar-Ponce JL, Arrieta O, González-Fierro A, Chávez-Blanco A, de la Cruz-Hernández E, Camargo MF, Trejo-Becerril C, Pérez-Cárdenas E, Pérez-Plasencia C, Taja-Chayeb L, Wegman-Ostrosky T, Revilla-Vazquez A, Dueñas-González A (2007) A phase II study of epigenetic therapy with hydralazine and magnesium valproate to overcome chemotherapy resistance in refractory solid tumors. Ann Oncol 18:1529–1538
44. Singh N, Dueñas-González A, Lyko F, Medina-Franco JL (2009) Molecular modeling and molecular dynamics studies of hydralazine with human DNA methyltransferase 1. ChemMedChem 4:792–799
45. Villar-Garea A, Fraga MF, Espada J, Esteller M (2003) Procaine is a DNA-demethylating agent with growth-inhibitory effects in human cancer cells. Cancer Res 63:4984–4989
46. Zhang J, Dong B, Zheng L, Li G (2006) Effect of procaine hydrochloride on the micellization of double tailed surfactants in the aqueous solution. Colloids Surf A 290:157–163
47. Brueckner B, Lyko F (2004) DNA methyltransferase inhibitors: old and new drugs for an epigenetic cancer therapy. Trends Pharmacol Sci 25:551–554
48. Lee BH, Yegnasubramanian S, Lin X, Nelson WG (2005) Procainamide Is a specific inhibitor of DNA methyltransferase 1. J Biol Chem 280:40749–40756
49. Fang MZ, Wang Y, Ai N, Hou Z, Sun Y, Lu H, Welsh W, Yang CS (2003) Tea polyphenol (-)-epigallocatechin-3-gallate inhibits DNA methyltransferase and reactivates methylation-silenced genes in cancer cell lines. Cancer Res 63:7563–7570
50. Gao Z, Xu Z, Hung MS, Lin YC, Wang T, Gong M, Zhi X, Jablon DM, You L (2009) Promoter demethylation of WIF-1 by epigallocatechin-3-gallate in lung cancer cells. Anticancer Res 29:2025–2030
51. Gu B, Ding Q, Xia G, Fang Z (2009) EGCG inhibits growth and induces apoptosis in renal cell carcinoma through TFPI-2 overexpression. Oncol Rep 21:635–640
52. Zaveri NT (2006) Green tea and its polyphenolic catechins: medicinal uses in cancer and noncancer applications. Life Sci 78:2073–2080
53. Medina-Franco JL, López-Vallejo F, Kuck D, Lyko F (2011) Natural products as DNA methyltransferase inhibitors: a computer-aided discovery approach. Mol Diversity 15:293–304
54. Jagadeesh S, Sinha S, Pal BC, Bhattacharya S, Banerjee PP (2007) Mahanine reverses an epigenetically silenced tumor suppressor gene RASSF1A in human prostate cancer cells. Biochem Biophys Res Commun 362:212–217
55. Sinha S, Pal BC, Jagadeesh S, Banerjee PP, Bandyopadhaya A, Bhattacharya S (2006) Mahanine inhibits growth and induces apoptosis in prostate cancer cells through the deactivation of Akt and activation of caspases. Prostate 66:1257–1265
56. Brueckner B, Garcia Boy R, Siedlecki P, Musch T, Kliem HC, Zielenkiewicz P, Suhai S, Wiessler M, Lyko F (2005) Epigenetic reactivation of tumor suppressor genes by a novel small-molecule inhibitor of human DNA methyltransferases. Cancer Res 65: 6305–6311
57. Schirrmacher E, Beck C, Brueckner B, Schmitges F, Siedlecki P, Bartenstein P, Lyko F, Schirrmacher R (2006) Synthesis and in vitro evaluation of biotinylated RG108: a high affinity compound for studying binding interactions with human DNA methyltransferases. Bioconjugate Chem 17:261–266
58. Siedlecki P, Garcia Boy R, Musch T, Brueckner B, Suhai S, Lyko F, Zielenkiewicz P (2006) Discovery of two novel, small-molecule inhibitors of DNA methylation. J Med Chem 49:678–683
59. Kuck D, Singh N, Lyko F, Medina-Franco JL (2010) Novel and selective DNA methyltransferase inhibitors: docking-based virtual screening and experimental evaluation. Bioorg Med Chem 18:822–829
60. Podvinec M, Lim SP, Schmidt T, Scarsi M, Wen D, Sonntag LS, Sanschagrin P, Shenkin PS, Schwede T (2010) Novel inhibitors of dengue virus methyltransferase: discovery by in vitro-driven virtual screening on a desktop computer grid. J Med Chem 53: 1483–1495
61. Schrump DS, Fischette MR, Nguyen DM, Zhao M, Li X, Kunst TF, Hancox A, Hong JA, Chen GA, Pishchik V, Figg WD, Murgo AJ, Steinberg SM (2006) Phase I study of decitabine-mediated gene expression in patients with cancers involving the lungs, esophagus, or pleura. Clin Cancer Res 12:5777–5785
62. Issa JP, Kantarjian HM, Kirkpatrick P (2005) Azacitidine. Nat Rev Drug Discov 4:275–276

63. Medina-Franco JL, Caulfield T (2011) Advances in the computational development of DNA methyltransferase inhibitors. Drug Discov Today 16:418–425
64. Consortium UniProt (2010) The Universal Protein Resource (UniProt) in 2010. Nucleic Acids Res 38:D142–D148
65. Siedlecki P, Garcia Boy R, Comagic S, Schirrmacher R, Wiessler M, Zielenkiewicz P, Suhai S, Lyko F (2003) Establishment and functional validation of a structural homology model for human DNA methyltransferase 1. Biochem Biophys Res Commun 306: 558–563
66. Dolan MA, Keil M, Baker DS (2008) Comparison of composer and ORCHESTRAR. Proteins: Struct Funct Bioinf 72:1243–1258
67. Laskowski RA, MacArthur MW, Moss DS, Thornton JM (1993) PROCHECK: a program to check the stereochemical quality of protein structures. J Appl Crystallogr 26:283–291
68. Macromodel, version 9.8, Schrödinger, LLC, New York, NY, 2010
69. Loving K, Salam NK, Sherman W (2009) Energetic analysis of fragment docking and application to structure-based pharmacophore hypothesis generation. J Comput-Aided Mol Des 23:541–554
70. Salam NK, Nuti R, Sherman W (2009) Novel method for generating structure-based pharmacophores using energetic analysis. J Chem Inf Model 49:2356–2368
71. Zhou L, Cheng X, Connolly BA, Dickman MJ, Hurd PJ, Hornby DP (2002) Zebularine: a novel DNA methylation inhibitor that forms a covalent complex with DNA methyltransferases. J Mol Biol 321:591–599
72. Kuttan G, Kumar KB, Guruvayoorappan C, Kuttan R (2007) Antitumor, anti-invasion, and antimetastatic effects of curcumin. Adv Exp Med Biol 595:173–184
73. Dueñas-González A, García-López P, Herrera LA, Medina-Franco JL, González-Fierro A, Candelaria M (2008) The prince and the pauper. A tale of anticancer targeted agents. Mol Cancer 7:82
74. Arce C, Segura-Pacheco B, Perez-Cardenas E, Taja-Chayeb L, Candelaria M, Dueñnas-Gonzalez A (2006) Hydralazine target: from blood vessels to the epigenome. J Transl Med 4:10
75. Lee WJ, Shim JY, Zhu BT (2005) Mechanisms for the inhibition of DNA methyltransferases by tea catechins and bioflavonoids. Mol Pharmacol 68:1018–1030
76. Evans DA, Bronowska AK (2009) Implications of fast-time scale dynamics of human DNA/RNA cytosine methyltransferases (DNMTs) for protein function. Theor Chem Acc 125:407–418